AIAA JOURNAL
Vol. 30, No. 3, March 1992

Effect of Structural Damping on Flutter of Plates with a Follower Force

Ken Higuchi*
Tokyo Denki University, Hatoyama, Hiki-gun, Saitama 350-03, Japan
and
Earl H. Dowell†
Duke University, Durham, North Carolina 27706

A plate-like large space structure may undergo dynamic instabilities when it is thrusted by a nonconservative compressive force. A flexible rectangular plate with four free edges, one of which is subjected to a tangential follower force, is considered. The effects of structural damping are studied here because small damping may destabilize the nonconservative system. The calculation shows that the thrusted free-edged plate with structural damping also has both divergence and flutter types of instability, and the flutter thrust load with small structural damping is drastically lower than that without damping. The destabilizing effect depends on the slenderness ratio of the rectangular plate.

Nomenclature

a = plate length
b = plate width
D = bending rigidity of plate, $Eh^3/[12(1 - \nu^2)]$
E = Young's modulus
h = plate thickness
$K_{1,mnij}$ = element of matrix K_1
$\overline{K_{1,mnij}}$ = element of nondimensional matrix K_1
$K_{2,mnij}$ = element of matrix K_2
$\overline{K_{2,mnij}}$ = element of nondimensional matrix K_2
$K_{3,mnij}$ = element of matrix K_3
$\overline{K_{3,mnij}}$ = element of nondimensional matrix K_3
M_{mnij} = element of mass matrix
$\overline{M_{mnij}}$ = element of nondimensional mass matrix
$\hat{m}$ = surface density, ρh
Q = nondimensional follower force
Q_F = nondimensional flutter load
Q_{ij} = generalized force
q = magnitude of a tangential follower force per unit width
T = kinetic energy
t = time
U = potential energy, $U_1 + U_2$
U_1 = strain energy due to plate bending
U_2 = strain energy to an in-plane compressive force
$\overline{W_{mn}}$ = see Eq. (25)
$W_{mn}(t)$ = generalized coordinate
w = plate deflection, $w(x,y,t)$
$X_m(x)$ = coordinate function in the x direction
x,y = coordinates
$Y_n(y)$ = coordinate function in the y direction
α = acceleration
α_F = flutter acceleration
γ = structural damping coefficient
δ = variation
$\hat{\delta}$ = Dirac's delta function
δW_D = virtual work done by a structural damping force
δW_F = virtual work done by an external follower force
δW_{NC} = virtual work done by nonconservative forces
η = nondimensional coordinate of y, y/b
λ = slenderness ratio, a/b
ν = Poisson's ratio
ξ = nondimensional coordinate of $x = x/a$
ρ = density
Ω = nondimensional frequency, $= \Omega_R + \Omega_I$
Ω_I = imaginary part of Ω
Ω_R = real part of Ω
ω = frequency
$\nabla^2(\ )$ = $\partial^2(\ )/\partial x^2 + \partial^2(\ )/\partial y^2$
$\dot{(\ )}$ = $\partial(\ )/\partial t$
$(\ )'$ = derivative with respect to a spatial coordinate

I. Introduction

A LARGE space structure may be constructed for low Earth orbit and then moved to a higher orbit by using a thruster. A plate-like large space structure, such as a solar power station, may undergo dynamic instabilities when it is thrusted because the rigidity of the structure is extremely low and because the thrust is a nonconservative compressive force.

The plate-like large space structure may be constructed as a truss structure with a large number of repeated unit space frames, and it often may be modeled as a continuous isotropic plate. A flexible rectangular plate with four free edges is considered here; one edge of the rectangular plate is subjected to a tangential follower force. The system is investigated by means of modal analysis.

The problem without any damping in the formulation was investigated by the authors.[1–3] The plate shows both flutter-type and divergence-type instabilities, and the critical value of the thrust load was obtained for various slenderness ratios of a rectangular flexible plate. The effects of structural damping are studied in the present paper. Generally, a large space structure is not damped quickly because the structure is very flexible and its frequency is extremely low, and so materials with large damping often are used intentionally or the vibration is controlled actively. However, small damping sometimes destabilizes a nonconservative system,[4–6] and this is the case here. The present result shows that the plate with struc-

Presented as Paper 90-0940 at the AIAA/ASME/ASCE/AHS/ASC 31st Structures, Structural Dynamics, and Materials Conference, Long Beach, CA, April 2-4, 1990; received Sept. 4, 1990; revision received March 27, 1991; accepted for publication March 29, 1991.

*Associate Professor, Faculty of Science and Engineering, Department of Industrial and Mechanical Engineering.

†Professor and Dean, School of Engineering, Department of Engineering and Materials Science.

tural damping also has both divergence and flutter types of instability, and the flutter thrust load with small structural damping is drastically lower than that without damping.

II. Formulation

An extended Hamilton's principle and a Rayleigh-Ritz approach[7] are applied to a flexible plate subjected to a pure tangential follower force (Fig. 1) as follows:

$$\delta \int_{t_1}^{t_2} (T - U + W_{NC})\, dt = 0 \tag{1}$$

where

$$T = \frac{1}{2} \int_0^b \int_0^a \hat{m} \dot{w}^2\, dx\, dy \tag{2}$$

$$U = U_1 + U_2 \tag{3}$$

$$\begin{aligned} U_1 &= \frac{1}{2} \int_0^b \int_0^a D \left[\left(\frac{\partial^2 w}{\partial x^2} + \nu \frac{\partial^2 w}{\partial y^2} \right) \frac{\partial^2 w}{\partial x^2} + \left(\frac{\partial^2 w}{\partial y^2} + \nu \frac{\partial^2 w}{\partial x^2} \right) \frac{\partial^2 w}{\partial y^2} + 2(1 - \nu) \left(\frac{\partial^2 w}{\partial x\, \partial y} \right)^2 \right] dx\, dy \\ &= \frac{1}{2} D \int_0^b \int_0^a \left\{ (\nabla^2 w)^2 + 2(1 - \nu) \times \left[\left(\frac{\partial^2 w}{\partial x\, \partial y} \right)^2 - \frac{\partial^2 w}{\partial x^2} \cdot \frac{\partial^2 w}{\partial y^2} \right] \right\} dx\, dy \end{aligned} \tag{4}$$

$$U_2 = -\frac{1}{2} \int_0^b \int_0^a q \frac{x}{a} \left(\frac{\partial w}{\partial x} \right)^2 dx\, dy \tag{5}$$

$$\delta W_{NC} = \delta W_F + \delta W_D \tag{6}$$

$$\delta W_F = -\int_0^b \int_0^a q \frac{\partial w}{\partial x} \hat{\delta}(x - a)\, \delta w\, dx\, dy \tag{7}$$

$$\delta W_D = -\frac{\gamma}{\omega} D \int_0^b \int_0^a \left[\left(\frac{\partial^2 \dot{w}}{\partial x^2} + \nu \frac{\partial^2 \dot{w}}{\partial y^2} \right) \delta \frac{\partial^2 w}{\partial x^2} + \left(\frac{\partial^2 \dot{w}}{\partial y^2} + \nu \frac{\partial^2 \dot{w}}{\partial x^2} \right) \delta \frac{\partial^2 w}{\partial y^2} + 2(1 - \nu) \frac{\partial^2 \dot{w}}{\partial x\, \partial y} \delta \frac{\partial^2 w}{\partial x\, \partial y} \right] dx\, dy \tag{8}$$

First, by introducing the expansion of the plate deflection $w(x,y,t)$ as

$$w(x,y,t) = \sum_m \sum_n W_{mn}(t) X_m(x) Y_n(y) \qquad m, n = 1, 2, 3, \ldots \tag{9}$$

we can rewrite T, U, and δW_{NC} by using coefficient matrices M_{mnij}, $K_{1,mnij}$, $K_{2,mnij}$, and $K_{3,mnij}$ as follows:

$$\begin{aligned} T &= \frac{1}{2} \int_0^b \int_0^a \hat{m} \sum_m \sum_n \sum_i \sum_j \dot{W}_{mn} \dot{W}_{ij} X_m Y_n X_i Y_j\, dx\, dy \\ &= \frac{1}{2} \hat{m} \sum_m \sum_n \sum_i \sum_j \dot{W}_{mn} \dot{W}_{ij} M_{mnij} \qquad m, n, i, j = 1, 2, 3, \ldots \end{aligned} \tag{10}$$

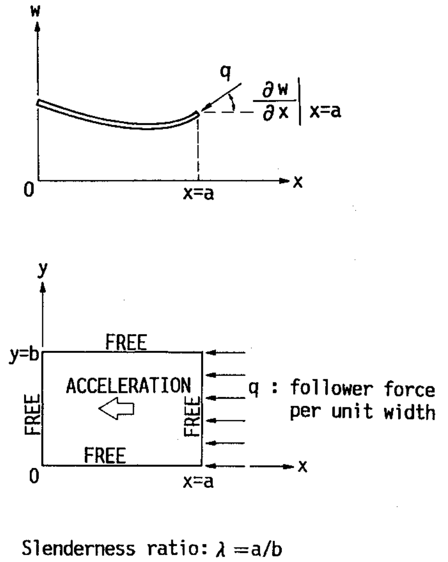

Fig. 1 Geometry of the model.

where

$$M_{mnij} = \int_0^b \int_0^a X_m Y_n X_i Y_j\, dx\, dy \qquad m, n, i, j = 1, 2, 3, \ldots \tag{11}$$

$$\begin{aligned} U_1 &= \frac{1}{2} D \int_0^b \int_0^a \sum_m \sum_n \sum_i \sum_j \times [(W_{mn} X''_m Y_n + \nu W_{mn} X_m Y''_n) W_{ij} X''_i Y_j + (W_{mn} X_m Y''_n + \nu W_{mn} X''_m Y_n) W_{ij} X_i Y''_j + 2(1 - \nu) W_{mn} X'_m Y'_n W_{ij} X'_i Y'_j]\, dx\, dy \\ &= \frac{1}{2} D \sum_m \sum_n \sum_i \sum_j W_{mn} W_{ij} K_{1,mnij} \end{aligned} \tag{12}$$

where

$$K_{1,mnij} = \int_0^b \int_0^a [(X''_m Y_n + \nu X_m Y''_n) X''_i Y_j + (X_m Y''_n + \nu X''_m Y_n) X_i Y''_j + 2(1 - \nu) X'_m Y'_n X'_i Y'_j]\, dx\, dy \tag{13}$$

$$\begin{aligned} U_2 &= -\frac{1}{2} \int_0^b \int_0^a q \frac{x}{a} \sum_m \sum_n \sum_i \sum_j \times W_{mn} X'_m Y_n W_{ij} X'_i Y_j\, dx\, dy \\ &= -\frac{1}{2} q \sum_m \sum_n \sum_i \sum_j W_{mn} W_{ij} K_{2,mnij} \end{aligned} \tag{14}$$

where

$$K_{2,mnij} = \int_0^b \int_0^a \frac{x}{a} X'_m Y_n X'_i Y_j\, dx\, dy \tag{15}$$

$$\begin{aligned} \delta W_F &= -\int_0^b \int_0^a q \sum_m \sum_n \sum_i \sum_j W_{mn} X'_m Y_n \hat{\delta}(x - a) \times \delta W_{ij} X_i Y_j\, dx\, dy \\ &= -q \sum_m \sum_n \sum_i \sum_j W_{mn} \delta W_{ij} K_{3,mnij} \end{aligned} \tag{16}$$

where

$$K_{3,mnij} = X'_m X_i \Big|_{x=a} \cdot \int_0^b Y_n Y_j \, dy \tag{17}$$

$$\delta W_D = -\frac{\gamma}{\omega} D \int_0^b \int_0^a \sum_m \sum_n \sum_i \sum_j \times [(\dot{W}_{mn} X''_m Y_n + \nu \dot{W}_{mn} X_m Y''_n)\, \delta W_{ij} X''_i Y_j + (\dot{W}_{mn} X_m Y''_n + \nu \dot{W}_{mn} X''_m Y_n)\, \delta W_{ij} X_i Y''_j + 2(1-\nu)\, \dot{W}_{mn} X'_m Y'_n \, \delta W_{ij} X'_i Y'_j] \, dx \, dy$$

$$= -\sum_m \sum_n \sum_i \sum_j \dot{W}_{mn} \delta W_{ij} C_{mnij} \tag{18}$$

where

$$C_{mnij} = \frac{\gamma}{\omega} D \int_0^b \int_0^a [(X''_m Y_n + \nu X_m Y''_n)\, X''_i Y_j + (X_m Y''_n + \nu X''_m Y_n)\, X_i Y''_j + 2(1-\nu)\, X'_m Y'_n X'_i Y'_j] \, dx \, dy$$

$$= \frac{\gamma}{\omega} D K_{1,mnij} \tag{19}$$

Therefore,

$$\delta W_D = -\frac{\gamma}{\omega} D \sum_m \sum_n \sum_i \sum_j \dot{W}_{mn} \delta W_{ij} K_{1,mnij} \tag{20}$$

One finds from Eqs. (19) that the damping matrix divided by $(\gamma/\omega)D$ is identical to the bending stiffness matrix.

Lagrange's equation has the form

$$\frac{d}{dt}\left[\frac{\partial(T-U)}{\partial \dot{W}_{ij}}\right] - \frac{\partial(T-U)}{\partial W_{ij}} = Q_{ij}$$

$$m, n, i, j = 1, 2, 3, \ldots \tag{21}$$

where

$$\delta W_{NC} = \sum_i \sum_j Q_{ij} \delta W_{ij} = \sum_i \sum_j \left(-q \sum_m \sum_n W_{mn} \delta W_{ij} K_{3,mnij} - \frac{\gamma}{\omega} D \sum_m \sum_n \dot{W}_{mn} \delta W_{ij} K_{1,mnij} \right) \tag{22}$$

Therefore,

$$Q_{ij} = -\sum_m \sum_n \left(q W_{mn} K_{3,mnij} + \frac{\gamma}{\omega} D \dot{W}_{mn} K_{1,mnij}\right)$$

$$m, n, i, j = 1, 2, 3, \ldots \tag{23}$$

T and U are given in Eqs. (10), (12), (14), and (3). Substituting these equations into Eq. (21), we obtain the equations of motion:

$$\sum_m \sum_n \left[\ddot{W}_{mn} \hat{m} M_{mnij} + \left(W_{mn} + \frac{\gamma}{\omega} \dot{W}_{mn} \right) D K_{1,mnij} + W_{mn}\, q(-K_{2,mnij} + K_{3,mnij}) \right] = 0$$

$$m, n, i, j = 1, 2, 3, \ldots \tag{24}$$

By assuming that the vibration is stationary, i.e.,

$$W_{mn}(t) = \overline{W_{mn}} \exp(i\omega t), \qquad i^2 = -1 \tag{25}$$

the equations of motion are reduced to the following eigenvalue equation for nontrivial solutions:

$$\det\{-\omega^2 \hat{m} [M_{mnij}] + D(1+i\gamma)[K_{1,mnij}] + q[-K_{2,mnij} + K_{3,mnij}]\} = 0 \tag{26}$$

We can use the functions of a free-free beam as the coordinate functions $X_m(x)$, $Y_n(y)$, $X_i(x)$, and $Y_j(y)$. Then, let us nondimensionalize the eigenvalue problem (26) by using

$$\xi = x/a \tag{27}$$

$$\eta = y/b \tag{28}$$

$$\lambda = a/b \tag{29}$$

Finally, we obtain a nondimensional eigenvalue problem as follows:

$$\det\{-\Omega^2 [\overline{M_{mnij}}] + (1+i\gamma)[\overline{K_{1,mnij}}] + Q[-\overline{K_{2,mnij}} + \overline{K_{3,mnij}}]\} = 0$$

$$m, n, i, j = 1, 2, 3, \ldots \tag{30}$$

where

$$\Omega^2 = \hat{m}\omega^2 a^4 / D \tag{31}$$

$$Q = q a^2 / D \tag{32}$$

are the nondimensional square frequency and the nondimensional load, respectively. Overbars in Eq. (30) denote nondimensionalized coefficient matrices.

III. Results and Discussion

A. Beam-Like Plate

A rectangular plate with a large slenderness ratio λ is a beam-like plate. It is shown in Ref. 1 that a plate with $\lambda = 10$ and $\nu = 0$ can be regarded as a beam in both its frequencies and its flutter loads. Eigenvalue curves for a beam-like plate with structural damping coefficient $\gamma = 0, 0.01, 0.05$ are shown in Figs. 2a and 2b. The ordinates Ω_R and Ω_I stand for real and imaginary parts of complex frequency Ω $(= \Omega_R + i\Omega_I)$, respectively.

Flutter for $\gamma = 0$ occurs when two real frequencies merge into a pair of conjugate complex frequency. In the case for $\gamma \neq 0$, frequencies are complex for all levels of load Q, and the two curves for the real part of the frequencies do not merge, but approach each other. Eigenvalue curves for $\gamma = 0$ are asymptotic curves for the case of $\gamma \neq 0$ both in real and in imaginary parts. Flutter for $\gamma \neq 0$ occurs when the imaginary part of a complex frequency changes from positive to negative because a negative imaginary part of a complex frequency makes the vibration amplitude diverge. Figure 2b shows that the imaginary part of eigenvalue curve for $\gamma \neq 0$ becomes negative at a lower load than that for $\gamma = 0$. That is, flutter with structural damping occurs at a lower load than that without damping.

The ratio of the imaginary part to the real part of complex frequency, Ω_I/Ω_R, is called the true damping ratio, and $-(\Omega_I/\Omega_R)$ characterizes the intensity of the flutter instability.[8] The ordinate of Fig. 3 shows the true damping ratio. The system is unstable dynamically if $\Omega_I/\Omega_R < 0$, and the condition $\Omega_I/\Omega_R = 0$ corresponds to neutral stability. All curves start from $\Omega_I/\Omega_R = \gamma/2$ at $Q = 0$ and approach the curve for $\gamma = 0$ asymptotically.

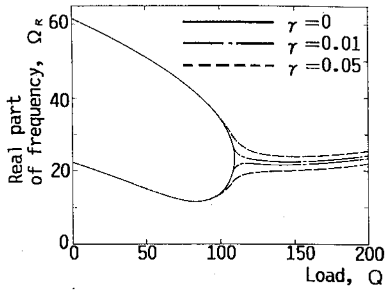

a) Real part of frequency

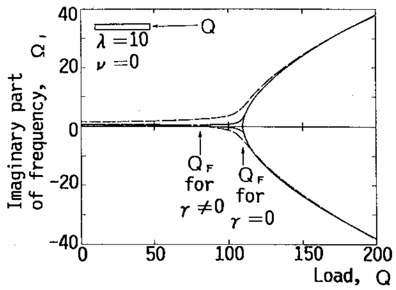

b) Imaginary part of frequency

Fig. 2 Complex frequency for load: slenderness ratio $\lambda = 10$; Poisson's ratio $\nu = 0$; structural damping coefficient: ——, $\gamma = 0$; —-—, $\gamma = 0.01$; ----, $\gamma = 0.05$.

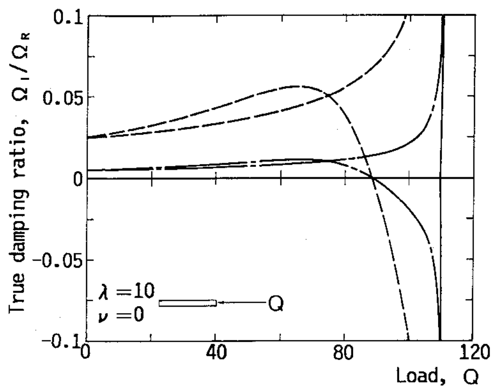

Fig. 3 Intensity of stability: $\lambda = 10$; $\nu = 0$; ——, $\gamma = 0$; —-—, $\gamma = 0.01$; ----, $\gamma = 0.05$.

The two curves cross the abscissa at almost the same value of load Q. It is easily seen that the flutter load Q_F for $\gamma \neq 0$ is insensitive to the change of γ. Figure 4 shows that Q_F for $\gamma \neq 0$ is almost constant and is drastically lower than that for $\gamma = 0$.

It is clear that the structural damping has a destabilizing effect on the nonconservative system of the free-free beam. The flutter load calculated from the assumption that damping is small and negligible is unconservative.

B. Rectangular Plate

The larger the slenderness ratio, the simpler the eigenvalue curve. Results for $\lambda = 2$, 1, and 0.5 are chosen here.

The eigenvalue curves in Fig. 5 for $\lambda = 2$ are comparatively simple. The lowest flutter for $\gamma \neq 0$ occurs at a lower load than at that for $\gamma = 0$, and so does the second lowest, as shown in Fig. 6.

For the case of a square plate, $\lambda = 1$, weak flutter instabilities appear as shown in Fig. 7. Flutter whose intensity is comparatively small and becomes stable or a decaying vibration with increasing Q is called a weak flutter. In Fig. 7, the lowest flutter load drops drastically if $\gamma \neq 0$. The second

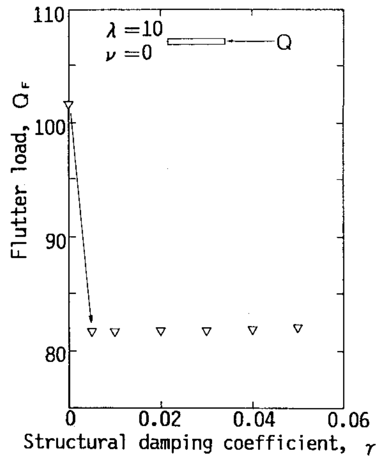

Fig. 4 Flutter load: $\lambda = 10$; $\nu = 0$.

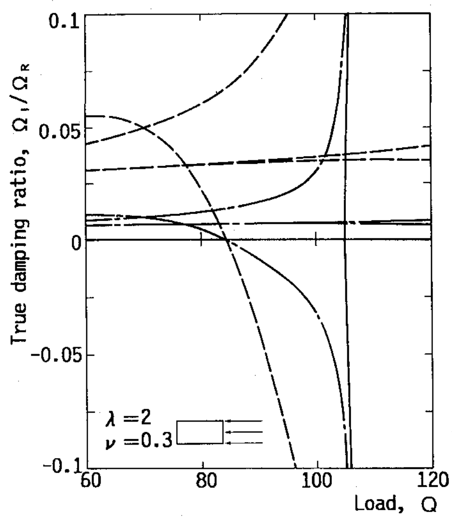

Fig. 5 Intensity of stability: $\lambda = 2$; $\nu = 0.3$; ——, $\gamma = 0$; —-—, $\gamma = 0.01$; ----, $\gamma = 0.05$.

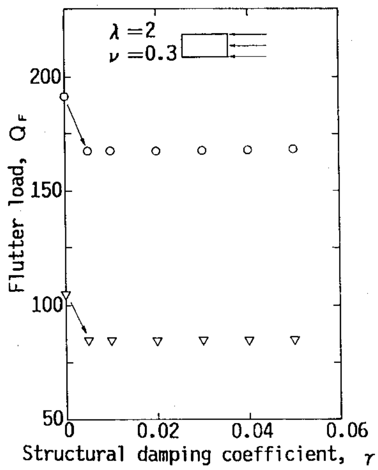

Fig. 6 Flutter load: $\lambda = 2$; $\nu = 0.3$; ▽, flutter of symmetric mode; ○, flutter of antisymmetric mode.

lowest flutter load also drops drastically if $\gamma \neq 0$, but its intensity becomes weak when $\gamma = 0.01$. The flutter becomes a weak flutter when $\gamma = 0.05$ and the load for the weak flutter becomes much larger. The intensity of the weak flutter becomes weaker and it disappears if γ is increased further. Figure 8 illustrates the behavior. Structural damping makes a weak flutter weaker and the weak flutter load larger.

Eigenvalue curves for $\lambda = 0.5$ in Fig. 9 are fairly complicated, and a weak flutter determines the critical load for this slenderness ratio. Weak flutter load and flutter load for various γ are shown in Fig. 10. Flutter for $\gamma \neq 0$ drops from the flutter load for $\gamma = 0$, but the change of the load is small.

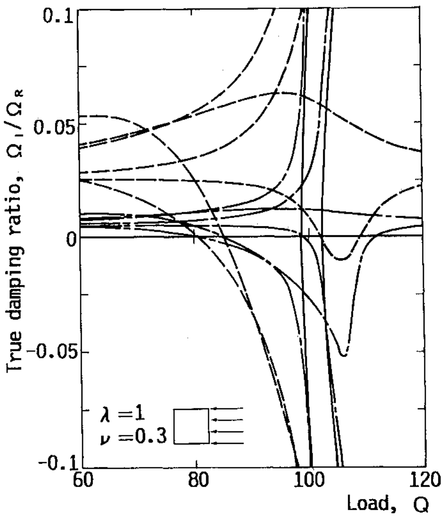

Fig. 7 Intensity of stability: $\lambda = 1$; $\nu = 0.3$; ——, $\gamma = 0$; — — —, $\gamma = 0.01$; ----, $\gamma = 0.05$.

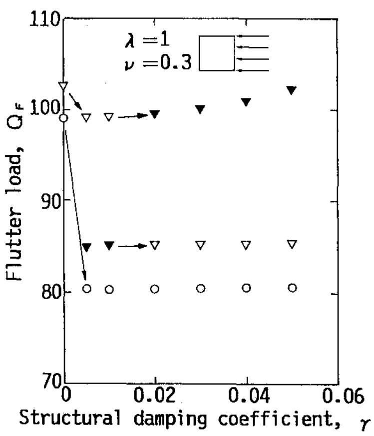

Fig. 8 Flutter load: $\lambda = 1$; $\nu = 0.3$; ▽, flutter of symmetric mode; ○, flutter of antisymmetric mode; ▼, weak flutter of symmetric mode.

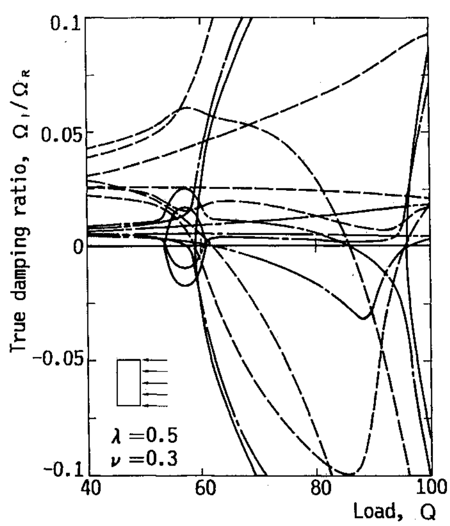

Fig. 9 Intensity of stability: $\lambda = 0.5$; $\nu = 0.3$; ——, $\gamma = 0$; — — —, $\gamma = 0.01$; ----, $\gamma = 0.05$.

Two weak flutter instabilities appear for a small γ; however, the weak flutter loads become larger gradually and the instabilities die out with increasing γ. The structural damping stabilizes weak flutter.

It is interesting to examine the results if one assumes that flutter occurs at a certain level of Ω_I/Ω_R whose level is not zero, but small and negative. The physical interest in considering a nonzero threshold for Ω_I/Ω_R is that one may show that a viscous damping term is equivalent to providing such a threshold.

Figure 11 shows the critical load for a plate with $\lambda = 1$ for various levels of a structural damping coefficient γ and for a threshold of the intensity of flutter, $-(\Omega_I/\Omega_R)$. The level of the nonzero threshold is chosen to be -0.001 in this figure. The critical load for flutter, which is determined from the condition that the level of threshold is -0.001, is changing continuously with the structural damping coefficient from $\gamma = 0$, although that determined from the condition of the zero threshold is almost constant regardless of the magnitude of γ ($\neq 0$) and is always lower than that for $\gamma = 0$. The difference in the flutter loads between the levels of threshold is attributed to the slope of the eigenvalue curve from the positive part to negative part of Ω_I/Ω_R. An eigenvalue curve with large γ crosses the abscissa, $\Omega_I/\Omega_R = 0$, with a steep slope, whereas a curve with small γ crosses the abscissa with shallower slope and comes closer to the curve for $\gamma = 0$. These facts are seen in Figs. 3, 5, and 7. A large structural damping, which causes a sudden instability due to increasing load, may not be recommended.

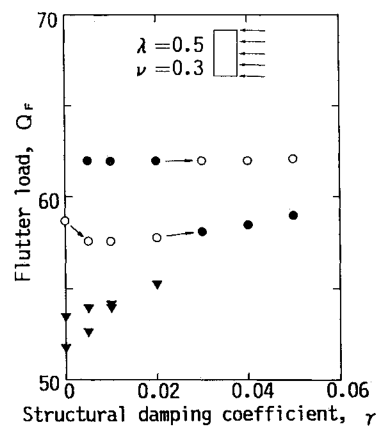

Fig. 10 Flutter load: $\lambda = 0.5$; $\nu = 0.3$; ○, flutter of antisymmetric mode; ●, weak flutter of antisymmetric mode; ▼, weak flutter of symmetric mode.

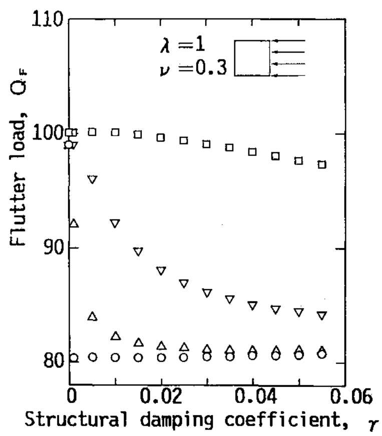

Fig. 11 Lowest flutter load for various levels of structural damping coefficient: $\lambda = 1$; $\nu = 0.3$; ○, $\Omega_I/\Omega_R = 0$; △, $\Omega_I/\Omega_R = -0.001$; ▽, $\Omega_I/\Omega_R = -0.01$; □, $\Omega_I/\Omega_R = -0.1$.

Divergence-type instability is also found, but the divergence load is much larger than the flutter load for the case $\lambda \geqq 0.5$.

The value of the nondimensional flutter load $Q_F \cong 80$ is practically meaningful. The acceleration of the plate is given by

$$\alpha = qa/\hat{m}ab = DQ/\hat{m}a^2b \tag{33}$$

For a given D, $\hat{m}$, a, b, the requirement that $Q < Q_F$ implies that $\alpha < \alpha_F$, where

$$\alpha_F = DQ_F/\hat{m}a^2b \tag{34}$$

Thus, there is a maximum acceleration α_F for a given plate due to the requirement that no flutter occurs.

As an example, consider $E = 7.0 \times 10^{10}[\mathrm{N/m^2}]$, $\nu = 0.3$, $\rho = 2.7 \times 10^3[\mathrm{kg/m^3}]$, $a = 1.0 \times 10^3[\mathrm{m}]$, $b = 5.0 \times 10^2[\mathrm{m}]$, and $h = 5.1 \times 10^{-2}[\mathrm{m}]$. Then

$$\alpha_F = 1.0 \times 10^{-2}[\mathrm{m/s^2}]$$

for $Q_F = 80$. This is only 1/1000 the acceleration of gravity on Earth. For thicker plates, note that $\alpha_F \sim h^2$. Hence, the maximum possible acceleration α_F may be increased by increasing the plate thickness h.

IV. Concluding Remarks

The effect of structural damping on the dynamic instability of a completely free plate subjected to a nonconservative follower force is studied.

1) Structural damping drastically destabilizes the strong flutter instabililty of the system considered here.

2) Structural damping stabilizes the weak flutter instability because it makes the weak instability weaker or suppresses flutter altogether.

3) The stabilizing and destabilizing effects of structural damping on the dynamic instability depend on the choice of slenderness ratio of the rectangular plate.

4) If viscous damping is included, the effect of structural damping on the flutter instability is less drastic. Viscous damping is always stabilizing.

Acknowledgment

This work was supported by a Grant-in-Aid for Encouragement of Young Scientists, the Ministry of Education, Science and Culture.

References

[1]Higuchi, K., and Dowell, E. H., "Dynamic Stability of a Rectangular Plate with Four Free Edges Subjected to a Follower Force," *AIAA Journal*, Vol. 28, No. 7, 1990, pp. 1300–1305; also *Proceedings of the AIAA/ASME/ASCE/AHS 29th Structures, Structural Dynamics, and Materials Conference*, Pt. 3, AIAA, Washington, DC, April 1988, pp. 1576–1583.

[2]Higuchi, K., and Dowell, E. H., "Effects of the Poisson Ratio and Negative Thrust on the Dynamic Stability of a Free Plate Subjected to a Follower Force," *Journal of Sound and Vibration*, Vol. 129, No. 2, 1989, pp. 255–269.

[3]Higuchi, K., and Dowell, E. H., "Dynamic Stability of a Completely Free Plate Subjected to a Controlled Non-Conservative Follower Force," *Journal of Sound and Vibration*, Vol. 131, No. 1, 1989, pp. 115–128.

[4]Herrman, G., and Jong, I. C., "On the Destabilising Effect of Damping in Nonconservative Elastic Systems," *Journal of Applied Mechanics*, Vol. 32, No. 3, 1965, pp. 592–597.

[5]Herrman, G., and Jong, I. C., "On Nonconservative Stability Problems of Elastic Systems with Slight Damping," *Journal of Applied Mechanics*, Vol. 33, No. 1, 1966, pp. 125–133.

[6]Ziegler, H., "Die Stabilitatskriterien der Elastomechanik," *Ingenieur-Archiv*, Vol. 20, 1952, pp. 49–56.

[7]Leipholz, H. H. E., and Pfendt, F., "Application of Extended Equations of Galerkin to Stability Problems of Rectangular Plates with Free Edges and Subjected to Uniformly Distributed Follower Forces," *Computer Methods in Applied Mechanics and Engineering*, Vol. 37, 1988, pp. 341–365.

[8]Dowell, E. H., Curtiss, H. C., Jr., Scanlan, R. H., and Sisto, F., *A Modern Course in Aeroelasticity*, Sijthoff & Noordhoff, Alphen aan den Rijn, The Netherlands, 1978, pp. 104–110.